On the structural transformation of Ni/BaH_2 during a N_2-H_2 chemical looping process for ammonia synthesis: a joint *in situ* inelastic neutron scattering and first-principles simulation study

Jisue Moon[1], Yongqiang Cheng[2], Luke Daemen[2], Eric Novak[2], Anibal J. Ramirez-Cuesta[2], Zili Wu[1*]

1. Chemical Science Division, 2. Neutron Scattering Division, Oak Ridge National Laboratory, Oak Ridge, TN 37831, USA

* Corresponding author: ZW, email: wuz1@ornl.gov

Abstract

The demand for decarbonizing the ammonia industry by using renewable energy has invoked increasing research interests into catalyst development for effective N_2 reduction under mild conditions. Hydride-based materials are among some of the emerging catalysts for ammonia synthesis at ambient pressure and low temperatures (<673 K). A recent chemical looping process based on Ni/BaH_2 showed the most promise as it can realize ammonia production at a temperature as low as 373 K and under ambient pressure. However, the chemical transformation of the hydride catalyst at the molecular level remains unclear in this process. In this work, we report detailed *in situ* neutron spectroscopy and diffraction investigations along with first-principles simulations on the structural transformation of Ni/BaH_2 during the nitridation and hydrogenation steps in the chemical looping process for ammonia synthesis. It was shown that a ball-milling process of the starting Ni/BaH_2 could significantly decrease the size of BaH_2 and increase the density of defects, thus potentially enhancing the reactivity of the hydride. The evolution from BaH_2 to barium imide (BaNH) was evidenced in the inelastic neutron scattering (INS) and neutron diffraction results during the N_2 reaction step. During the hydrogenation study, in addition to the recovery of BaH_2, a possible intermediate species, N-deficient barium imide, was also detected. In comparing the N_2 and H_2 reaction steps, the neutron results indicate that the hydrogenation step is more difficult than the nitridation step, confirming the facile N_2 fixation property of Ni/BaH_2 catalyst in ammonia synthesis.

Keywords: chemical looping, ammonia synthesis, Ni/BaH_2, neutron scattering, first-principles simulations

Introduction

As a crucial component in fertilizers, ammonia is also a promising carrier for hydrogen storage because of its high volumetric and gravimetric hydrogen densities and potential as clean fuel for fuel cells and combustion engines.[1,2] Traditionally, a Haber-Bosch (HB) process is used as the main industrial route for ammonia production in which nitrogen and hydrogen gases react catalytically under harsh operating temperatures (673-873 K) and pressure (20-40 MPa), consuming 1~2% of world annual energy output.[3-6] Because ammonia synthesis at low temperatures is thermodynamically favorable, new catalytic processes have been explored for ammonia synthesis in a more sustainable and environmentally benign way, i.e., under much milder conditions than the HB process. Recent notable progress in heterogeneous catalysis has been witnessed in the utilization of advanced materials including nitrides,[7,8] electrides,[9,10] hydrides[11-14] including oxyhydrides[14,15] as the catalysts or supports, which enabled ammonia synthesis at temperatures below 673 K and at ambient pressure.

Among the emerging catalysts, alkali and alkaline hydride-based materials hold great promise in ammonia synthesis due to their appreciable reaction rate at mild conditions.[4-6] For example, the Chen group showed the first example of using hydrides such as LiH as co-catalysts working synergistically with transition metals including Cr, Mn, Fe and Co for ammonia synthesis at 423 – 623 K that outperformed the Cs-promoted Ru catalyst, one of the most active NH_3 synthesis catalysts by 2—3 times at 573 K and 12—20 times at 523 K.[11] Recently, a chemical looping process comprised of nitrogen fixation and hydrogenation steps over Ni/BaH_2 was demonstrated by the same group for ammonia synthesis at a temperature as low as 373 K and atmospheric pressure with the rate more than one order of magnitude higher than that of the commercial catalyst (Cs-Ru/MgO).[16] In these studies based on alkali and alkaline hydrides, the facile transformation among imides (NH^{2-}), amide (NH_2^-), and hydrides (H^-) plays an essential role in the N-H bond formation and NH_3 production. NHx hydrogenation was considered the rate-limiting step (RDS) over these hydrides instead of the N_2 activation step on traditional ammonia synthesis catalysts.[11] For example, in the chemical looping process, it was proposed (see **Figure 1**) that the hydride anion in BaH_2 is a strong reducing agent and has a chemical potential that drives the N fixation step by providing electrons to N_2 to break the triple bond of N_2 and to form the imide intermediate (BaNH). During the hydrogenation step, the hydrogen undergoes disproportionation to hydridic and protic H atoms to bond with Ba and nitrogen atoms to form

BaH_2 and ammonia, respectively.[16] Interestingly, the physically mixed late 3d metal (such as Ni, Co, and Fe) with metal hydride increases its N_2 dissociation/hydrogenation ability, up to 6 times higher than the metal hydride itself [16,12], indicating a synergism between the hydride and the metal components. Although the role of metal hydride has been studied to understand the kinetics beyond the nitrogen fixation and hydrogenation steps of the chemical looping process, there is still a lack of understanding of the mechanism at the molecular level via spectroscopy by *in situ* monitoring the cycling between the metal hydride and imide species, and any potential intermediates during the looping process.

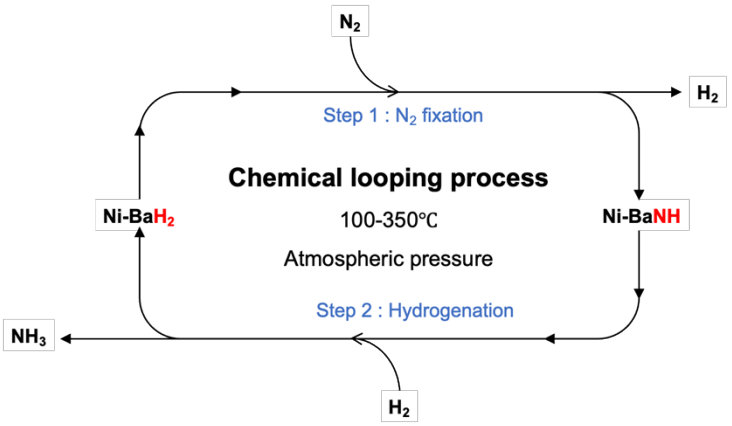

Figure 1. The proposed mechanism for the Chemical looping process for ammonia synthesis over Ni/BaH_2, modified from Ref. [16].

Neutron scattering is highly sensitive to hydrogen compared to other scattering techniques such as X-ray or electron scattering. It has been demonstrated as a powerful tool to probe the molecular structure of alkali and alkaline hydride, imide, and amide species via neutron diffraction and especially inelastic neutron scattering (INS).[9,17-22] Taking advantage of neutron scattering techniques and using Ni/BaH_2 as a model catalyst, this work aims to elucidate the detailed mechanism of the chemical transformation of BaH_2 in the N_2-H_2 chemical looping process using both INS and neutron diffraction. First-principles calculations combined with lattice and molecular dynamic simulations are employed to interpret the neutron spectroscopy results and to understand the structures and their dynamics. It is clearly shown that both stoichiometric and non-stoichiometric BaH_2 and BaNH species are involved during the cycling process for ammonia synthesis. The result provides additional insights into the structural dynamics of hydride-based catalysts in the chemical looping process for ammonia synthesis.

Experimental

Barium hydride (American Elements, 99.7 % metal basis) and nickel powder (Sigma-Aldrich, nanopowder <100nm, >99% trace metals basis) were used as received. The mixture of

nickel powder and barium hydride were prepared via ball milling at a ratio of 1:1 (2 g of BaH_2 and 2 g of Ni powder). The powders were mixed in a glass vial and the resulting mixture was placed in a vial with tungsten carbide caps and one steel ball for ball-milling with a high-energy SPEX mill. All operations were conducted in a dry helium glove box (H_2O < 0.1 ppm, O_2 < 0.1 ppm). Ball-milling was performed overnight (~18 hr), alternating between 30 minutes periods of ball-milling and 5 minutes of cooling time (no ball-milling), corresponding to just under 16 hours of ball-milling time. X-Ray diffraction (XRD) experiments of the samples before and after ball milling were performed using a PANalytical X'Pert Pro MPD diffractometer with Cu-Kα radiation (λ = 1.5418 Å). The ball-milled sample was recovered and placed in an aluminum sample holder for the following neutron scattering experiment.

INS experiments were performed at the VISION beamline (BL-16B) of Spallation Neutron Source (SNS) at Oak Ridge National Laboratory. An empty aluminum can was measured at 5 K to collect the background of the INS spectrum. The Ni/BaH_2 sample (4 g) was then loaded in the can and further exposed to 393 K under vacuum to remove the remaining moisture in the sample. After such treatment, the blank sample was measured at 5 K. After measurement, the sample was heated to 573 K and exposed to 3 bar of N_2 at 573 K for 2 hr. The sample was then pumped shortly to remove any gaseous hydrogen-containing species at 573 K and exposed to 3 bar of N_2 for an additional 2 hr at the same temperature. The sample was shortly pumped at 573 K to remove any gaseous and adsorbed species and then cooled down to 373 K and further pumped down to base vacuum level. After such treatment, the sample was cooled down to 5 K to collect the INS spectrum. The sample was further exposed to 3 bar of H_2 at 573 K for 2 hr and then shortly pumped at 573 K and cooled down to room temperature followed by pumping down to remove unreacted H_2. It was quenched to 5 K to collect the INS spectrum. Neutron diffraction patterns were also collected for the sample during the measurement of the INS spectra. All gas loading operations at the neutron beam line were performed *in situ* with the sample undisturbed in the sample holder, which allows potential quantitative analysis of the hydrogen content in the sample during the different steps.

First-principles simulations including lattice dynamics (LD) and molecular dynamics (MD) simulations were conducted using Vienna Ab initio Simulation Package (VASP).[23] The calculation used Projector Augmented Wave (PAW) method [24,25] to describe the effects of core electrons, and Perdew-Burke-Ernzerhof (PBE) [26] implementation of the Generalized

Gradient Approximation (GGA) for the exchange-correlation functional. The energy cutoff was 500 eV for the plane-wave basis of the valence electrons. The lattice parameters and atomic coordinates from the literature were used as the initial structure. The total energy tolerance for electronic energy minimization was 10^{-8} eV, and for structure optimization it was 10^{-7} eV. The maximum interatomic force after relaxation was below 0.005 eV/Å. The vibrational eigen-frequencies and modes were then calculated by solving the force constants and dynamical matrix using Phonopy.[27] The OClimax software[28] was used to convert the DFT-calculated phonon results to the simulated INS spectra. MD simulations were performed with a lower cutoff energy (400 eV), at 300 K, with a time step of 1.0 fs.

Results and Discussion

Impact of ball milling on the structure of Ni/BaH_2

It was shown by the Chen group [16] that adding nickel nanoparticles (NPs) to BaH_2 can not only lower the onset temperature in both the nitridation and hydrogenation steps, but also increase the reaction rates in both steps, especially the nitridation step (up to 30 times) relative to the bare BaH_2 in the chemical looping process. These promotional effects were attributed to the addition of Ni functionality, which was introduced via the ball milling process. However, in addition to creating intimate contact between Ni NPs and BaH_2, it is unclear if ball milling plays an extra role for example in impacting the structure of BaH_2. In this context, we first investigate the INS spectra of Ni/BaH_2 with and without the ball milling procedure and the results are shown in **Figure 2A**.

The spectrum from a simple physical mixture of Ni/BaH_2 shows several sharp peaks below 1050 cm^{-1} with a few broad features above 1100 cm^{-1}, similar to what was reported for well-crystallized BaH_2.[29] The sharp peaks can be divided into two regions as marked as A (400 – 700 cm^{-1}) and B (700 – 1100 cm^{-1}) in the spectra due to the vibrational modes of two types of hydrides in BaH_2 lattice. The lower energy branch A is associated with the vibrations of the 5-coordinated H (denoted as H_A site) in an approximate square-pyramidal structure. In contrast, branch B is due to the vibrations of the 4-coordinated H (denoted as H_B site) in a tetragonal structure, as shown in the illustration in **Figure 2B.** The subpeaks in each branch are due to the rattling of the hydride ions along different directions. Similar to previous work[29], the LD simulated spectrum matches generally well with that of the crystalline BaH_2 but some discrepancies exist especially in the A

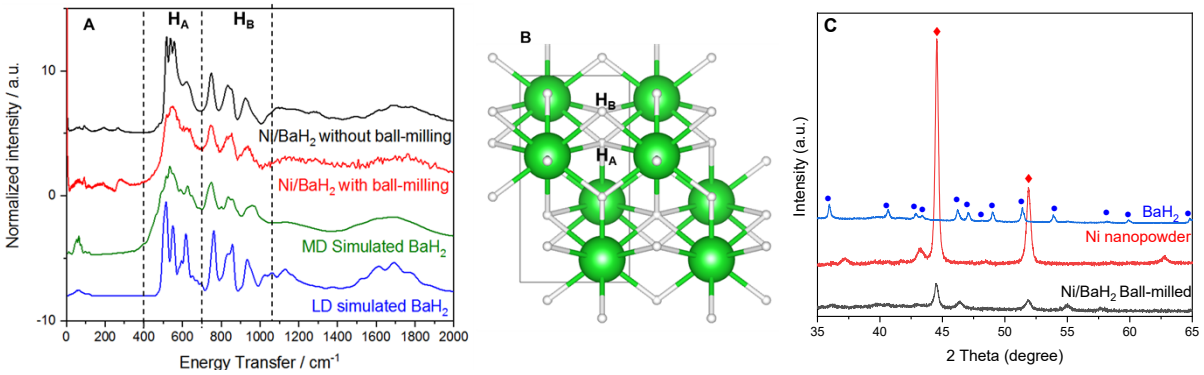

Figure 2. (A) INS spectra of Ni/BaH_2 before and after ball milling. The LD and MD simulated BaH_2 spectra are also shown for comparison. (B) Illustration of the two types hydride ions in the BaH_2 structure. Green ball: Ba; white ball: H. (C) XRD patterns of BaH_2, Ni nanopowder and ball-milled Ni/BaH_2.

branch region, likely due to the complex local potential energy profile and anharmonicity associated with the 5-coordinated H. MD simulation was further employed to probe the potential energy profile and the trajectory was converted to simulated INS spectrum. As shown in **Figure 2A**, compared to the LD simulation, the spectral features including relative peak intensity and frequency from MD simulation are now closer to those in the measured spectra from BaH_2, indicating that anharmonicity indeed plays a role, at least for the 5-coordinated H. The peaks from the MD simulation are also generally broader than those observed in the experiment, probably due to the higher temperature used in the simulation which was intended to partially include the zero-point energy fluctuation of H atoms, while using a classical model, but would also introduce artifacts caused by larger Ba displacements (equivalent to more disorder Ba coordinates).

The INS spectrum from Ni/BaH_2 after ball milling shows similar spectral contour to that of the physical mixture. Still, with a significant peak broadening, a spectral feature very similar to that of the MD simulated one. This interesting observation indicates that the ball milling process results in a breakdown of the particle size and disordering of the BaH_2 and thus less crystallinity. This is confirmed by the XRD patterns (**Figure 2C**) collected before and after ball milling: the size of BaH_2 decreases significantly from 78 to 27 nm. Such a change can lead to increased defects in BaH_2 and thus can enhance its chemical reactivity, potentially an additional contributing factor to the improved performance of Ni/BaH_2 in the chemical looping process in ammonia synthesis in addition to the role of Ni NPs. Other possible contributing factors for the peak broadening include the formation of Ni hydride or BaNi hydride species during the high energy ball milling process.

Unfortunately, some of the major peaks from Ni hydride[30] and presumed bimetallic BaNi hydrides would be buried under the features from BaH_2 and thus cannot be identified definitely. Furthermore, the neutron diffraction patterns (reported below) do not show clear evidence for the potential presence of these hydrides after the ball milling. Thus, it is not likely that new hydride species are formed during the ball milling process, and the INS spectral profile (broadening) change is mostly related to the size change and creation of defects in BaH_2.

Neutron diffraction patterns collected during the INS experiment also support the change occurred to Ni/BaH_2 during ball milling. As shown in **Figure 3.** the diffraction peaks at ~2.61, 3.22, 3.40 and 3.65 Å due to BaH_2 are apparently broadened after the ball milling process. Notably, new peaks are observed at 1.60, 1.95, and 2.75 Å after ball milling. These peaks are identified to be due to BaO. It is possible that the trace water or O_2 (<0.1 ppm) in the glove box system slowly oxidizes a portion of BaH_2 to BaO during the long ball milling process (~18 hr). Such a BaO phase also seems to be present in the XRD pattern of Ni/BaH_2 reported by Chen and coworkers [16] (maybe in different amount from our case). Since the peaks due to the BaO phase only become sharper during the cycling process due to the annealing effect, it does not seem that BaO plays any

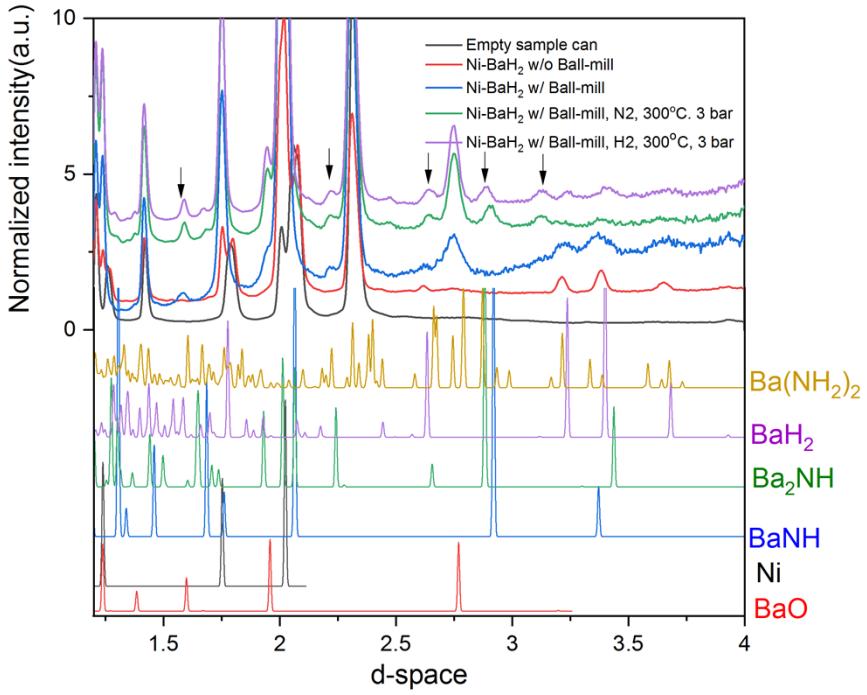

Figure 3. neutron diffraction patterns collected for Ni/BaH_2 with and without ball milling, and during the N_2-H_2 cycling process. The peaks from several standards including $Ba(NH_2)_2$, BaH_2, Ba_2NH, BaNH, Ni, and BaO are also shown at the bottom.

role in the chemical looping process. Instead, BaH_2 is the major player, as shown by the changes of the neutron diffraction peaks and the INS spectra (shown below) during the cycling process.

Structural changes in the N_2 reaction step

Figure 4A shows the INS spectra of ball-milled Ni/BaH_2 before and after a nitridation step at 573 K after different reaction times. Because of the INS cell configuration, i.e., the contact of gases with the sample is in a stationary mode, 3 bar of N_2 was used to facilitate the reaction instead of the typically used ambient pressure in the chemical looping.[16] After 1 hr reaction, some 20% intensity decline is observed for the spectrum from Ni/BaH_2, indicating the consumption of BaH_2. After 4 hr reaction, a significant change in spectral intensity is observed, suggesting a successful reaction between N_2 and Ni/BaH_2 has occurred. The most likely reaction between N_2 and BaH_2 (R1) was proposed previously[16] as follows:

$$2BaH_2 + N_2 \rightarrow 2BaNH + H_2 \qquad \text{R1}$$

Indeed, a subtraction of the INS spectra before (scaled down to match the intensity in the A and B branch regions) and after the N_2 reaction step (4 hr data) results in a spectrum with features similar to that of reported barium imide (BaNH) [19] which is also plotted in **Figure 4B**, implying the formation of BaNH species in the nitridation step over Ni/BaH_2, consistent with the previous observation from X-ray diffraction [16]. The modes associated with the major INS bands of the imide species are illustrated in **Figure 4C**. Interestingly, the intensity decline from the two types of hydride sites, H_A and H_B, does not show the evident difference after either 1 or 4 hr reaction in N_2, indicating a similar reactivity of the two types of lattice hydrides towards N_2 in Ni/BaH_2.

In the corresponding neutron diffraction patterns shown in **Figure 3,** a few extra diffraction peaks appear at ~1.68, 2.22, 2.64, 2.88, and 3.12 Å after the N_2 reaction step. The simulated patterns from BaH_2, BaNH, Ba_2NH and $Ba(NH_2)_2$ are also included for comparison. Apparently, BaNH and BaH_2 can account for most of the peaks, confirming the formation of BaNH in the nitridation step. Noticeably, the diffraction intensity decreases after the N_2 reaction step and regains after the H_2 step, which is indicative of H abstraction and addition into the sample since the neutron diffraction intensity is mostly from the incoherent scattering of hydrogen atoms.

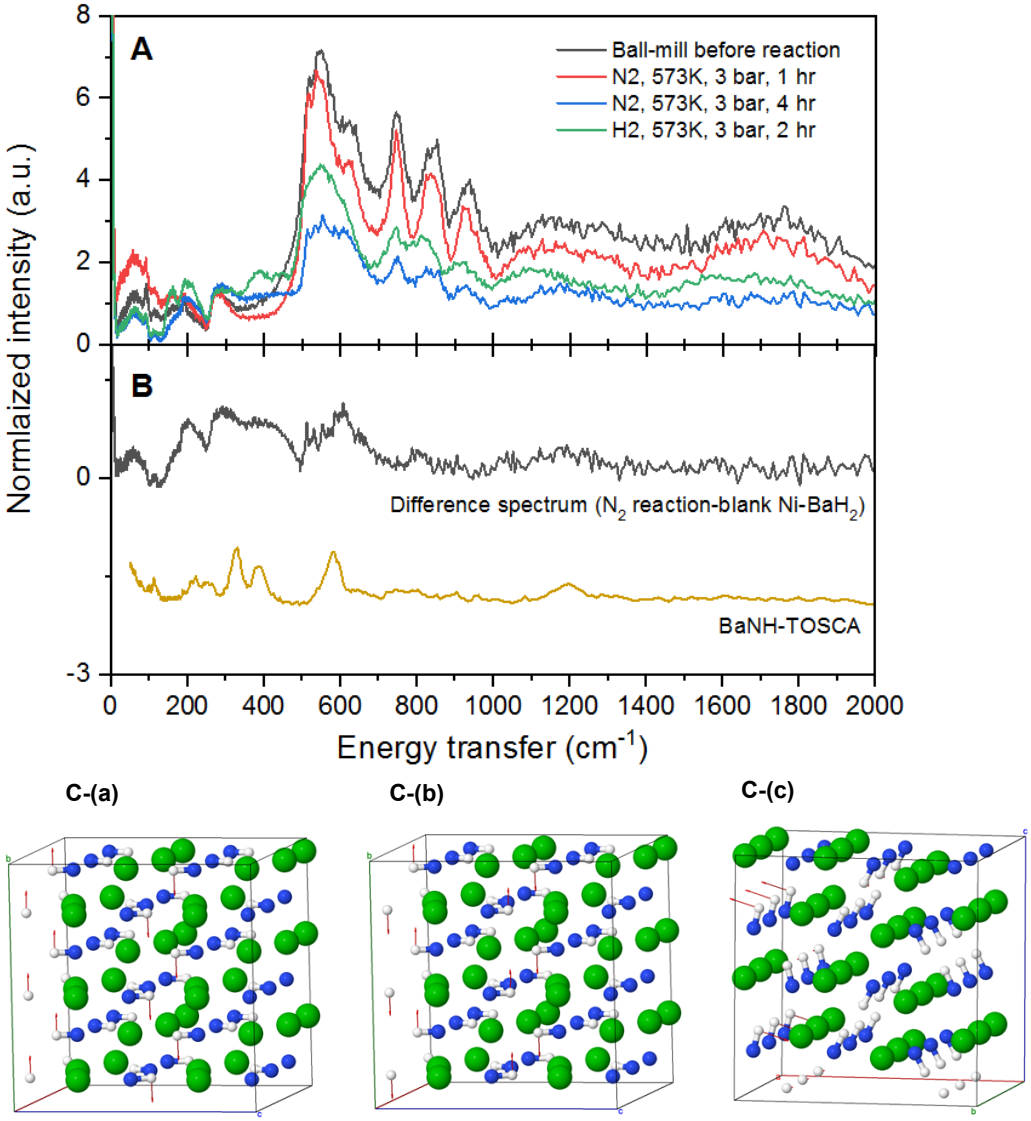

Figure 4. A) INS spectra of Ni/BaH_2 before reaction, after N_2 reaction for 1 and 4 hr at 573 K, and after H_2 reaction for 2 hr at 573 K. B) comparison of difference INS spectrum after N_2 reaction with that reported for BaNH. C) Illustration of representative vibrational modes in BaNH for the INS bands at (a) 200, (b) 350, and (c) 600 cm^{-1}. Green ball: Ba; Blue ball: N; while ball: H.

Structural changes in the H_2 reaction step

The INS spectrum from H_2 reaction step after the N_2 step over Ni/BaH_2 is also included in **Figure 4A**. An obvious increase in the spectral intensity is noted relative to the spectrum after N_2 reaction, suggesting the incorporation of hydrogen species into the sample. Considering the

concomitant increase of intensity in the A and B branches in the spectrum, the formation of BaH_2 can be expected from the hydrogenation of imide as the following:

$$BaNH + 2H_2 \rightarrow BaH_2 + NH_3 \quad \text{R2}$$

However, the spectral features are somewhat different from the starting BaH_2, implying potential formation of new species in addition to BaH_2 during the hydrogenation step. A difference spectrum is obtained to identify such new species by subtracting the spectrum (after H_2 reaction) from the one after N_2 reaction (scaled to similar intensity) and plotted in **Figure 5A**. The main features from 500 to 1200 cm^{-1} are similar to those of BaH_2, again confirming barium hydride production from imide hydrogenation. It is notable that the peak positions are slightly different from those of pure BaH_2 (**Figure 2A**), likely due to a modified local potential around H sites in BaH_2 in the chemical looping process. Yet the presence of some extra spectral features below 500 cm^{-1} not found in BaH_2 spectrum suggests the formation of new species during the imide hydrogenation. Considering amide is a possible intermediate in the hydrogenation of imide to hydride (see reactions R3-R4), the INS spectra from $Ba(NH_2)_2$ are compared with the obtained difference spectrum in **Figure 5A**.

$$2BaNH + 2H_2 \rightarrow Ba(NH_2)_2 + BaH_2 \quad \text{R3}$$

$$Ba(NH_2)_2 + 2H_2 \rightarrow BaH_2 + 2NH_3 \quad \text{R4}$$

However, even though the reported spectrum of $Mg(NH_2)_2$[31] matches fairly well in the region below 500 cm^{-1} with the features from the new species formed during the H_2 step, the simulated spectrum from $Ba(NH_2)_2$ (no experimentally measured spectrum available in the literature) does not resemble well. We then turn to the neutron diffraction pattern to examine the changes after H_2 reaction. The most obvious change is a systematic shift of the BaNH diffraction peaks to a lower d-spacing, by about 0.7%. A possible explanation of this shift is the formation of N- deficient barium imide, $BaN_{1-x}H_{1+y}$ ($0 \leq x\ (y) \leq 1$), as H_2 can react away some of the N to form NH_3, and the imide is in a defective intermediate state as it is eventually converted to BaH_2. An interesting reference to compare with is Ba_2NH, which has a similar Ba arrangement as in BaNH but with some of the N and proton removed as illustrated in **Figure 5B**, resulting in a smaller average Ba-Ba distance and therefore a shift of the corresponding Bragg peaks to lower d- spacing (**Figure 3**). In our case, as BaNH is reacted with H_2, some of the N will be released (with protons, in the form of NH_3), and the added H will be in the form of H^-, forming hydride with Ba. We believe such a similar local environment as in Ba_2NH will lead to reduced lattice constants, and

this intermediate phase $BaN_{1-x}H_{1+y}$ ($0 \leq x$ (y) ≤ 1) is likely what we have observed in the neutron diffraction.

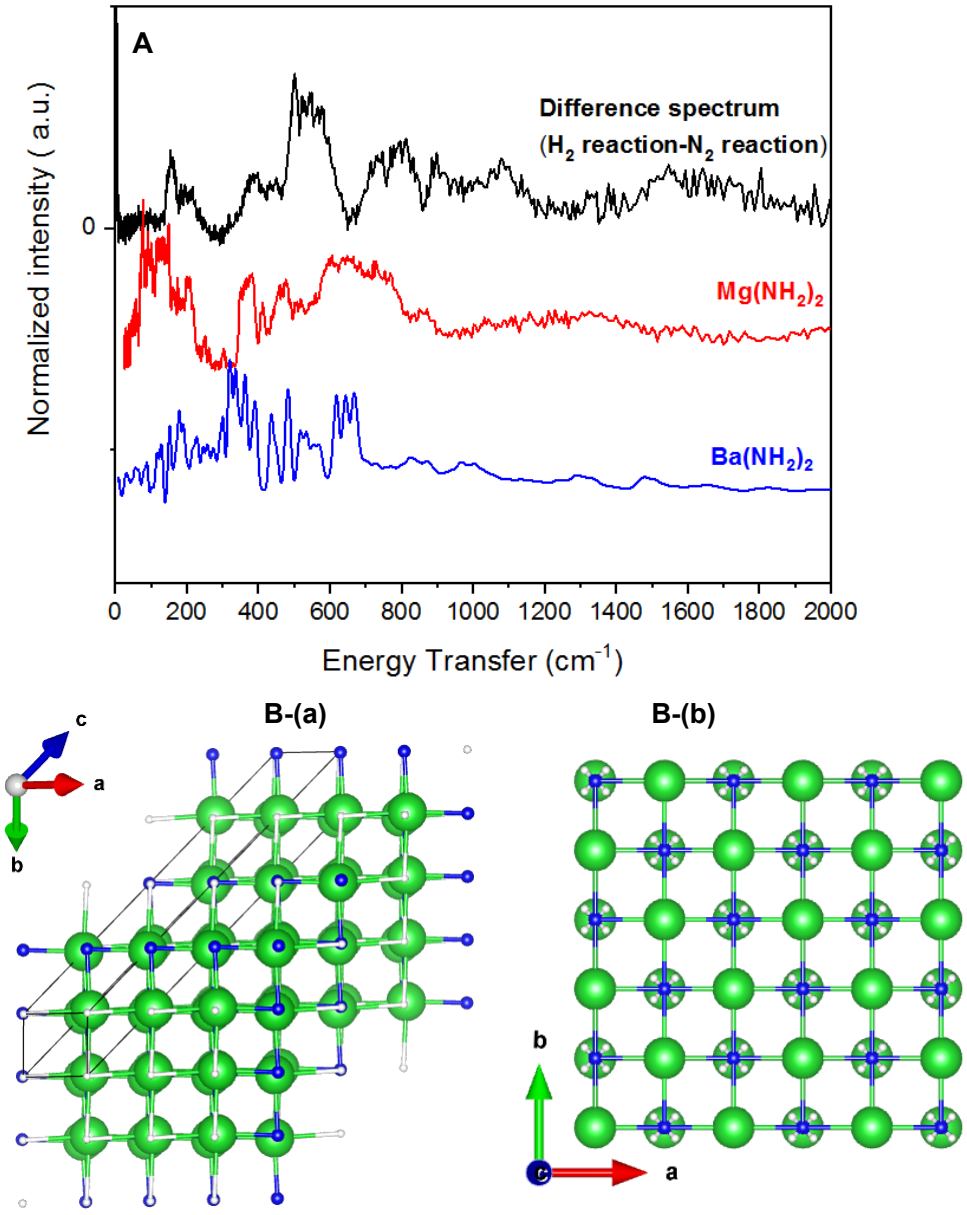

Figure 5. A). INS difference spectrum subtracted from H_2 step from N_2 step over Ni/BaH_2. The reported INS spectrum of $Mg(NH_2)_2$ and simulated spectrum of $Ba(NH_2)_2$ are also shown for comparison. B) Crystal structures of (a) Ba_2NH and (b) BaNH. This angle of view highlights the similarity between the two in terms of the overall rock-salt-like arrangement of Ba and N. The differences are mainly the occupancy of the N site, as well as the position and valence state of H. Green ball: Ba; Blue ball: N; while ball: H.

The formation of N-deficient barium imide intermediate was not observed in the previous study of chemical looping for ammonia synthesis using X-ray diffraction[16]. The contrast can be attributable to the different reaction conditions used in our neutron study and the high sensitivity of neutron spectroscopy to hydrogenous species, especially when the species is not fully crystallized. The observation of the mixture of BaH_2 and possible $BaN_{1-x}H_{1+y}$ ($0 \leq x$ (y) ≤ 1) in the hydrogenation step along with the not fully restored intensity of the INS spectrum (compared with the original BaH_2 one), indicates that the hydrogenation step could be more difficult than the nitridation step. This is consistent with previous kinetic studies of ammonia synthesis over BaH_2-supported transition metals where the N-H hydrogenation rather than the N_2 activation was considered the rate-limiting step for ammonia synthesis.[12] Of note, the coexistence of H_2 and NH_3 in the batch reactor used in our neutron study might also play a role for the incomplete hydrogenation of BaNH.

Conclusions

The chemical looping process for ammonia synthesis over Ni/BaH_2 was monitored by *in situ* neutron spectroscopy and neutron diffraction to reveal the structural evolution of BaH_2 during the different steps. The interpretation of the INS spectra was assisted with first-principles simulations, including lattice dynamics and molecular dynamics simulations. The neutron results exhibited that the ball-milling process, even though producing some BaO phase that was shown to be a spectator for ammonia synthesis, can significantly reduce the crystalline size of BaH_2 and thus potentially increase its reactivity in ammonia synthesis. The transformation from BaH_2 to BaNH was successfully monitored by both INS and neutron diffraction during the N_2 reaction step. The reverse to BaH_2 was also evidenced by INS during the H_2 step, while a likely intermediate phase, N-deficient barium imide, was also indicated by both INS and neutron diffraction. The incomplete hydrogenation of imide to hydride seems to imply that the hydrogenation of NHx species is more difficult than the N_2 fixation (nitridation) step, consistent with the reported kinetic studies over Ni/BaH_2 for chemical looping production of ammonia.

Acknowledgements

This research is sponsored by the Laboratory Directed Research Development (LDRD) of Oak Ridge National Laboratory, managed by UT-Battelle, LLC, for the U.S. Department of Energy. ZW was partly supported by the U.S. Department of Energy, Office of Science, Office of Basic Energy Sciences, Chemical Sciences, Geosciences, and Biosciences Division, Catalysis Science program. The neutron studies were conducted at the Spallation Neutron Source, a DOE Office of Science User Facility operated by the Oak Ridge National Laboratory. Part of the sample preparation was conducted at the Center for Nanophase Materials Sciences, a DOE Office of Science User Facility.

Declarations

The authors declare no competing financial interest.

References

1. Klerke A, Christensen CH, Nørskov JK, Vegge T (2008) Ammonia for hydrogen storage: challenges and opportunities. Journal of Materials Chemistry 18 (20):2304-2310. doi:10.1039/B720020J
2. Lan R, Irvine JTS, Tao S (2012) Ammonia and related chemicals as potential indirect hydrogen storage materials. International Journal of Hydrogen Energy 37 (2):1482-1494. doi:https://doi.org/10.1016/j.ijhydene.2011.10.004
3. Chen JG, Crooks RM, Seefeldt LC, Bren KL, Bullock RM, Darensbourg MY, Holland PL, Hoffman B, Janik MJ, Jones AK, Kanatzidis MG, King P, Lancaster KM, Lymar SV, Pfromm P, Schneider WF, Schrock RR (2018) Beyond fossil fuel–driven nitrogen transformations. Science 360 (6391):eaar6611. doi:10.1126/science.aar6611 %J Science
4. Marakatti VS, Gaigneaux EM (2020) Recent Advances in Heterogeneous Catalysis for Ammonia Synthesis. ChemCatChem 12 (23):5838-5857. doi:https://doi.org/10.1002/cctc.202001141
5. Wang Q, Guo J, Chen P (2019) Recent progress towards mild-condition ammonia synthesis. Journal of Energy Chemistry 36:25-36. doi:https://doi.org/10.1016/j.jechem.2019.01.027
6. Gao W, Guo J, Chen P (2019) Hydrides, Amides and Imides Mediated Ammonia Synthesis and Decomposition. Chinese Journal of Chemistry 37 (5):442-451. doi:https://doi.org/10.1002/cjoc.201800586
7. Kojima R, Aika K-i (2001) Cobalt molybdenum bimetallic nitride catalysts for ammonia synthesis: Part 2. Kinetic study. Applied Catalysis A: General 218 (1):121-128. doi:https://doi.org/10.1016/S0926-860X(01)00626-3
8. Ye T-N, Park S-W, Lu Y, Li J, Sasase M, Kitano M, Tada T, Hosono H (2020) Vacancy-enabled N2 activation for ammonia synthesis on an Ni-loaded catalyst. Nature 583 (7816):391-395. doi:10.1038/s41586-020-2464-9

9. Kammert J, Moon J, Cheng Y, Daemen L, Irle S, Fung V, Liu J, Page K, Ma X, Phaneuf V, Tong J, Ramirez-Cuesta AJ, Wu Z (2020) Nature of Reactive Hydrogen for Ammonia Synthesis over a Ru/C12A7 Electride Catalyst. Journal of the American Chemical Society 142 (16):7655-7667. doi:10.1021/jacs.0c02345
10. Hara M, Kitano M, Hosono H (2017) Ru-Loaded C12A7:e– Electride as a Catalyst for Ammonia Synthesis. ACS Catalysis 7 (4):2313-2324. doi:10.1021/acscatal.6b03357
11. Wang P, Chang F, Gao W, Guo J, Wu G, He T, Chen P (2017) Breaking scaling relations to achieve low-temperature ammonia synthesis through LiH-mediated nitrogen transfer and hydrogenation. Nature Chemistry 9 (1):64-70. doi:10.1038/nchem.2595
12. Gao W, Wang P, Guo J, Chang F, He T, Wang Q, Wu G, Chen P (2017) Barium Hydride-Mediated Nitrogen Transfer and Hydrogenation for Ammonia Synthesis: A Case Study of Cobalt. ACS Catalysis 7 (5):3654-3661. doi:10.1021/acscatal.7b00284
13. Chang F, Guan Y, Chang X, Guo J, Wang P, Gao W, Wu G, Zheng J, Li X, Chen P (2018) Alkali and Alkaline Earth Hydrides-Driven N2 Activation and Transformation over Mn Nitride Catalyst. Journal of the American Chemical Society 140 (44):14799-14806. doi:10.1021/jacs.8b08334
14. Kobayashi Y, Tang Y, Kageyama T, Yamashita H, Masuda N, Hosokawa S, Kageyama H (2017) Titanium-Based Hydrides as Heterogeneous Catalysts for Ammonia Synthesis. Journal of the American Chemical Society 139 (50):18240-18246. doi:10.1021/jacs.7b08891
15. Tang Y, Kobayashi Y, Masuda N, Uchida Y, Okamoto H, Kageyama T, Hosokawa S, Loyer F, Mitsuhara K, Yamanaka K, Tamenori Y, Tassel C, Yamamoto T, Tanaka T, Kageyama H (2018) Metal-Dependent Support Effects of Oxyhydride-Supported Ru, Fe, Co Catalysts for Ammonia Synthesis. Advanced Energy Materials 8 (36):1801772. doi:https://doi.org/10.1002/aenm.201801772
16. Gao W, Guo J, Wang P, Wang Q, Chang F, Pei Q, Zhang W, Liu L, Chen P (2018) Production of ammonia via a chemical looping process based on metal imides as nitrogen carriers. Nature Energy 3 (12):1067-1075. doi:10.1038/s41560-018-0268-z
17. Polo-Garzon F, Luo S, Cheng Y, Page KL, Ramirez-Cuesta AJ, Britt PF, Wu Z (2019) Neutron Scattering Investigations of Hydride Species in Heterogeneous Catalysis. ChemSusChem 12 (1):93-103. doi:10.1002/cssc.201801890
18. Pietropaolo A, Colognesi D, Catti M, Nale AC, Adams MA, Ramirez-Cuesta AJ, Mayers J (2012) Proton vibrational dynamics in lithium imide investigated through incoherent inelastic and Compton neutron scattering. The Journal of Chemical Physics 137 (20):204309. doi:10.1063/1.4767566
19. Eβmann R, Jacobs H, Tomkinson J (1993) Neutron vibrational spectroscopy of imide ions (NH2−) in bariumimide (BaNH). Journal of Alloys and Compounds 191 (1):131-134. doi:https://doi.org/10.1016/0925-8388(93)90284-T
20. David WIF, Jones MO, Gregory DH, Jewell CM, Johnson SR, Walton A, Edwards PP (2007) A Mechanism for Non-stoichiometry in the Lithium Amide/Lithium Imide Hydrogen Storage Reaction. Journal of the American Chemical Society 129 (6):1594-1601. doi:10.1021/ja066016s
21. Ramirez-Cuesta AJ, Jones MO, David WIF (2009) Neutron scattering and hydrogen storage. Materials Today 12 (11):54-61. doi:https://doi.org/10.1016/S1369-7021(09)70299-8
22. Parker SF, Lennon D, Albers PW (2011) Vibrational Spectroscopy with Neutrons: A Review of New Directions. Applied Spectroscopy 65 (12):1325-1341. doi:10.1366/11-06456

23. Kresse G, Furthmüller J (1996) Efficient iterative schemes for ab initio total-energy calculations using a plane-wave basis set. Physical Review B 54 (16):11169-11186. doi:10.1103/PhysRevB.54.11169
24. Blöchl PE (1994) Projector augmented-wave method. Physical Review B 50 (24):17953-17979. doi:10.1103/PhysRevB.50.17953
25. Kresse G, Joubert D (1999) From ultrasoft pseudopotentials to the projector augmented-wave method. Physical Review B 59 (3):1758-1775. doi:10.1103/PhysRevB.59.1758
26. Perdew JP, Burke K, Ernzerhof M (1996) Generalized Gradient Approximation Made Simple. Physical Review Letters 77 (18):3865-3868. doi:10.1103/PhysRevLett.77.3865
27. Togo A, Tanaka I (2015) First principles phonon calculations in materials science. Scripta Materialia 108:1-5. doi:https://doi.org/10.1016/j.scriptamat.2015.07.021
28. Cheng YQ, Daemen LL, Kolesnikov AI, Ramirez-Cuesta AJ (2019) Simulation of Inelastic Neutron Scattering Spectra Using OCLIMAX. Journal of Chemical Theory and Computation 15 (3):1974-1982. doi:10.1021/acs.jctc.8b01250
29. Colognesi D, Barrera G, Ramirez-Cuesta AJ, Zoppi M (2007) Hydrogen self-dynamics in orthorhombic alkaline earth hydrides through incoherent inelastic neutron scattering. Journal of Alloys and Compounds 427 (1):18-24. doi:https://doi.org/10.1016/j.jallcom.2006.03.031
30. Antonov VE, Ivanov AS, Kuzovnikov MA, Tkacz M (2013) Neutron spectroscopy of nickel deuteride. Journal of Alloys and Compounds 580:S109-S113. doi:https://doi.org/10.1016/j.jallcom.2013.03.021
31. http://wwwisis2.isis.rl.ac.uk/INSdatabase/Results.asp?Magnesiumamide.